Sub-aperture Method for the Wide-Bandwidth Wide-Angle Inverse Synthetic Aperture Radar Imaging

Caner OZDEMİR[1], Ozkan KIRIK[1], Betül YILMAZ[1]

[1]Mersin University, Dept. of Electrical-Electronics Engineering Mersin University Ciftlikkoy 33343, Mersin, Turkey
cozdemir@mersin.edu.tr, ozkan@mersin.edu.tr, betuly@mersin.edu.tr

Abstract

In this paper, a method for obtaining focused inverse synthetic aperture radar (ISAR) images of targets based on the radar backscattering measurements taken over wide bands and wide angles [1]. The proposed method divides wide angle and wide frequency band into small aperture bands in the spatial frequency or Fourier domain. This set-up makes it possible to use fast calculation of ISAR images for every sub-aperture data set as in the case of standard ISAR case of small-bandwidth and small-angle. The details of the method are presented and numerical examples are given for the validation the method. The electromagnetic scattering estimation from the target is calculated via a hybrid simulator that uses both the physical optics [1-3] and the shooting & bouncing ray concepts [4].

1. Introduction

Inverse Synthetic Aperture Radar (ISAR) is a powerful signal processing technique for imaging moving targets in range and cross-range domains [5, 6]. The usual way of getting two-dimensional ISAR images in down-range and cross-range domains is to collect the frequency and aspect diverse backscattered field data from the target [5]. For the monostatic arrangement, the back scattered data over frequencies and angles occupies a two dimensional data grid in the spatial-frequency domain (or in the $k_x - k_y$ plane) as illustrated in Fig. 1. In ISAR applications, the common practice is to collect the data in small frequency bandwidth and in narrow angular bandwidth. This selection makes it possible to use fast algorithms such as fast Fourier transform (FFT) in forming the final ISAR image (Fig.2). It is also worthwhile to point out that the down-range resolution is inversely proportional the frequency bandwidth and the cross-range resolution is inversely proportional the aspect bandwidth. Therefore; although the selection of small angular and frequency bandwidth makes it possible to fast formation of the ISAR image, the resolutions in down and cross ranges cannot be improved much. Furthermore, operation of radar within a narrow look-angle bandwidth can only provide information about the scattering centers from that looking angle, and other hot-point areas that could be imaged from other look angles cannot be show up in the ISAR image. For all these reasons, there is a need for finding an effective way of forming the ISAR image for wide-frequency and wide-angle measurements. With this construct, the following advantages will be attained: (i) Since the resolution in the image domain will be much better, the image quality will also be much better, (ii) since the radar illuminates the target from a wider look-angle, the outline of the target in the ISAR image will be more apparent. This in turn; of course, will provide better information in recognizing and classifying the target. In most of the real-world scenarios where the collected data is provided for large angles, i.e. larger than 5° in practice, the small-angle approximations cannot be readily used. Therefore, there is a need for a fast and effective technique for displaying good-quality ISAR images for the data collected for angles larger than the small-angle approximation is not valid.

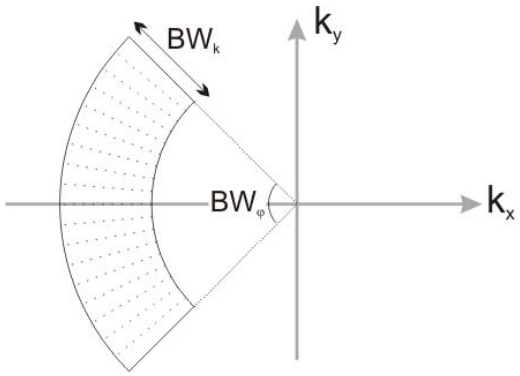

Fig. 1. Collection of ISAR raw data in Fourier Domain [5]

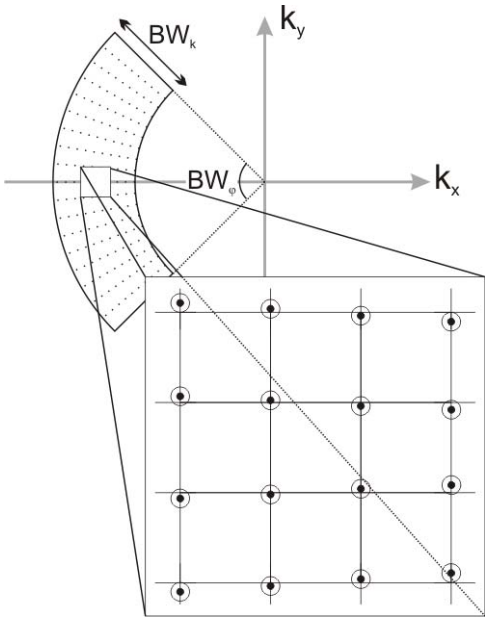

Fig. 2. Small band and small angle raw data over grid

In this work, we are proposing a simple, but an effective method for forming ISAR images of targets by using wide-angle wide-bandwidth backscattered field data. The details of the

algorithm are presented and numerical examples that illustrate the effectiveness of the proposed method are given.

2. Sub-aperture Method for Wide-Angle Wide-Bandwidth ISAR imaging

For the traditional operation of ISAR, it is usually preferable to work with small frequency bandwidth and small bandwidth of look-angles for the reasons mentioned above. When these conditions are not met, i.e., the frequency bandwidth is not small compared to center frequency of operation and the look-angles are wide, then the data set do not lie on a rectangular grid on the two dimensional (2D) Fourier plane. Therefore, it is not possible to use fast Fourier transform (FFT) in calculating the ISAR image. If this is the case, usually a polar to rectangular transformation is done to form the data set on a Cartesian grid [7-9].

2.1 The Algorithm of the method

Our approach of getting a focused image for the wide-band, wide-angle ISAR imaging is somewhat different than the usual approaches. In this alternative method, the disk-like data portion on the Fourier or $k_x - k_y$ plane is divided into small areas that look like rectangular portions as seen in Fig.3 (a). The steps of the algorithm are then summarized as follows:

(i) Collect the data for a wide range of frequencies and look-angles and record the complex backscattered field value as $E^s(f, \emptyset)$. If all 360° azimuth angles are covered, the data set will be a ring in the Fourier domain as depicted in Fig. 3(a).

(ii) Divide the data set in the $k_x - k_y$ space into MxN sub data set that is almost rectangular in the Fourier domain as illustrated in Fig. 3(a). Here, M represents the division ratio along the frequencies and N represents the division ratio along the angles.

(iii) Apply FFT routine to get each sub image. At this stage, we have a total of MxN ISAR image for different center frequencies and different look-angles. This stage is demonstrated in the Fig. 3(b).

(iv) Transform each sub-ISAR image from its own local coordinate system to global coordinates. At this stage, an interpolation scheme has to be applied, since the transformed grid generally will not be uniform in the global coordinate system (see Fig. 3(c)).

(v) Finally, sum up all transformed sub-ISAR images to get the final focused ISAR image as depicted in Fig. 3(d).

2.1. Signal processing aspects of the method

While applying the above algorithm, several signal processing aspects have to be carefully applied as they are listed in order:

(i) While dividing the whole block of data set into MxN times small data set, the new data set should satisfy the small-bandwidth small-angle approximation. This is the requirement for fast formation of the ISAR images by the help of FFT. Therefore, the center frequency of the each sub-data set should be at least ten times larger than the frequency bandwidth. Similarly, the angular bandwidth should be selected to be lower than at most 6° in azimuth.

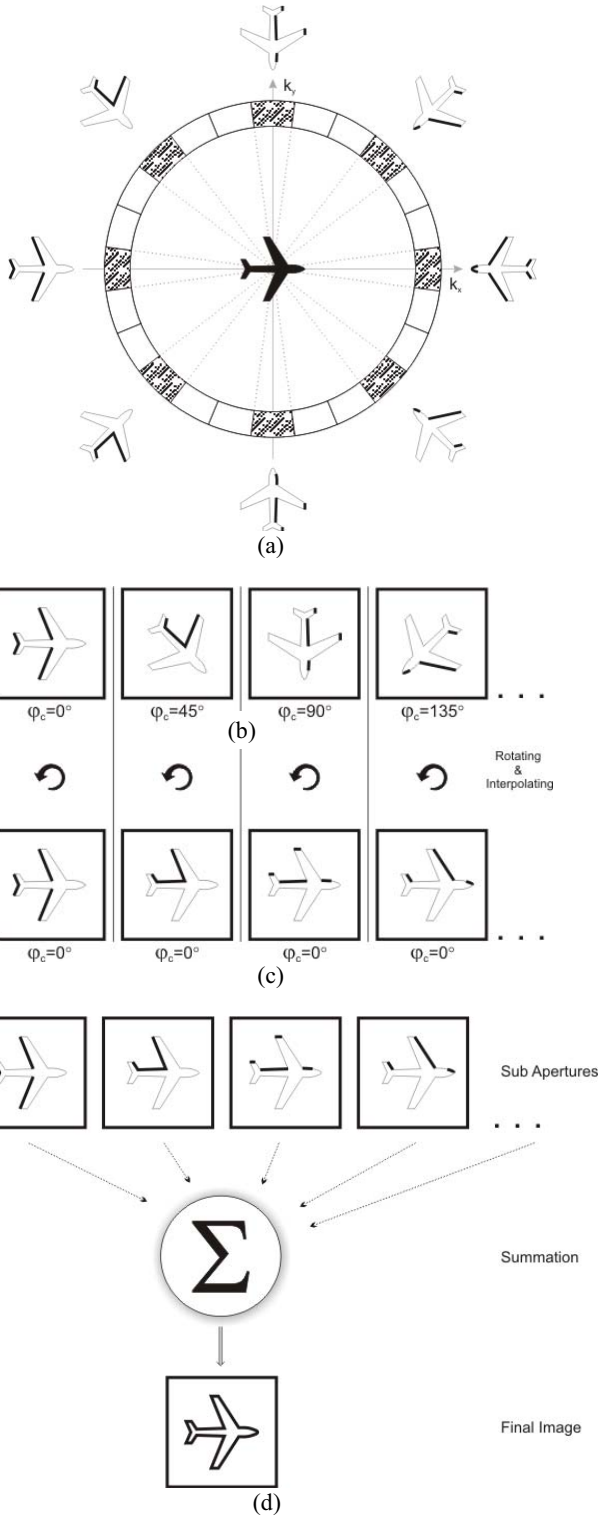

Fig. 3. (a) The backscattered field data is collected in wide-angles, (b) FFT based ISAR image generation for each sub-data set, (c) transforming all sub-images from their own local coordinate system to global coordinates, (d) summing up all sub-image in the global x-y plane to form the final ISAR image

(ii) After getting sub-ISAR images after FFT, a coordinate transformation is needed since the down-range and the cross-range axis of each sub-ISAR image is different. Cartesian to Polar transformation applied to image. Therefore, each sub-image should be rotated in the azimuth direction by the value of its center azimuth angle.

(iii) After rotating the image pixel in the local coordinate system to the global coordinate system, the transformed images will not lie on a uniformly reference image's grid because of the nature of the Polar-to-Cartesian transformation. Therefore, an interpolation scheme has to be applied to be able to sum all sub-ISAR images. The common interpolation scheme for this type of application is the *nearest neighbor interpolation* (NNI) [11].

The process of interpolation using first order NNI is demonstrated via Fig.4: If A_P is the amplitude of a pixel point P and r_1, r_2, r_3 and r_4 are the distances from point P to the nearest grid points, then these grid points are updated according to their distances from the original data point as follows:

$$R = \frac{1}{r_1} + \frac{1}{r_2} + \frac{1}{r_3} + \frac{1}{r_4}$$
$$A_1 = A_P/(r_1.R)$$
$$A_2 = A_P/(r_2.R)$$
$$A_3 = A_P/(r_3.R)$$
$$A_4 = A_P/(r_4.R) \quad (1)$$

After this interpolation, the new data set is uniformly sampled in the global down-range cross-range plane such that the image matrix is ready for summing operation.

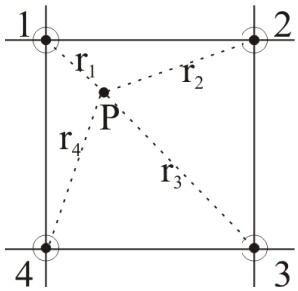

Fig. 4. The first-order, nearest neighbor interpolation [7]

(iv) As commonly applied in most SAR/ISAR applications, applying a prior windowing function such as Hanning [10] or Kaiser [12] does filter out either measured or numerical noise.

(v) Now all sub-ISAR image matrixes at same dimensions. Finally, sum up all matrixes to obtain final image.

3. Numerical Example

The success of the proposed technique was tested using a numerical example. An airplane whose CAD model is shown in Fig.5 is selected as the target. The electromagnetic (EM) simulation of this target was carried out via a high frequency EM simulator that used the both the physical optics and the shooting and bouncing ray (SBR) techniques [4]. This code can predict EM scattering from large and complex objects at high frequencies with good fidelities.

During the simulation, frequency was varied from $6.65\ GHz$ to $7.34\ GHz$ with 64 equally spaced frequency steps. Also, the azimuth angle was altered from 0° to 360° with 0,0879° angular incremental steps to get 4096 different angle points. Therefore, we had a total of 4096 backscattered raw data points after the simulation. Then, the proposed method was applied to be able form the wide-angle ISAR image of the model airplane. Applied steps of the algorithm are the followings:

(i) The angle bandwidth was selected as $BW_{\emptyset} = 5.625°$ for the sub-data set to satisfy the small angle requirement. This selection provided a total of 64 different sub-data set each having $64x64$ raw data value.

(ii) Using regular small-angle small-bandwidth ISAR imaging scheme [13,14], 64 different ISAR image of the airplane model was get by taking the 2-D FFT of the each of 64 different sub-data set. While applying the inversion, a *Hanning* type windowing scheme [10] was employed. Some $64x64$ ISAR images were displayed in Fig.6 where the ISAR images for the look-angles of 0°, 45°, 90° and 135° from the nose of the airplane were shown in order.

(iii) Rotation and the interpolation procedures were applied as explained in the above algorithm. For the NNI application, the down-range and cross-range pixel granularity were selected as $54{,}68\ mm$ and $54{,}68\ mm$ respectively. The rotated and interpolated versions of the ISAR images in Fig. 6 were displayed in Fig. 7 where all images were aligned in the same down-range cross-range plane.

(iv) Finally, all these aligned sub-ISAR images were summed up to form the final, focused ISAR image as shown in Fig.8.

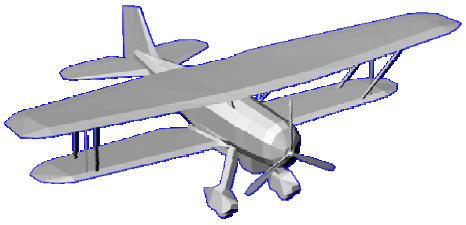

Fig. 5. Three dimensional CAD model of a airplane to get the wide-angle ISAR image at high frequencies

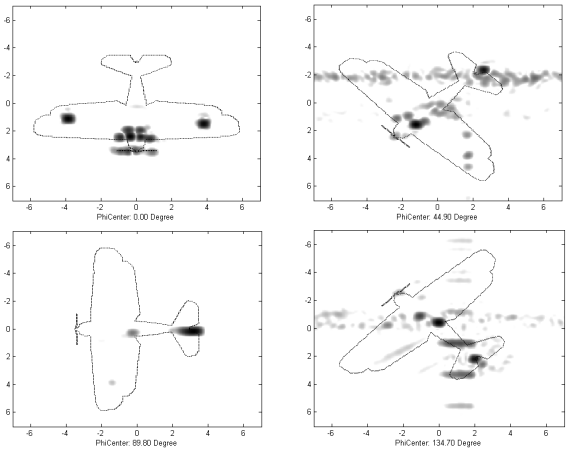

Fig. 6. Some selected ISAR images for different look-angles

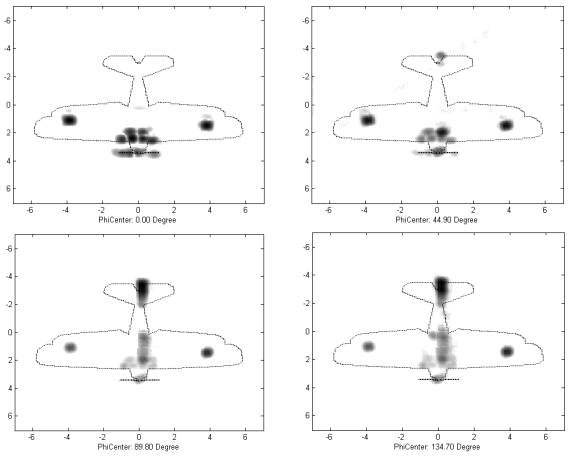

Fig. 7. Aligned ISAR images after rotation and interpolation

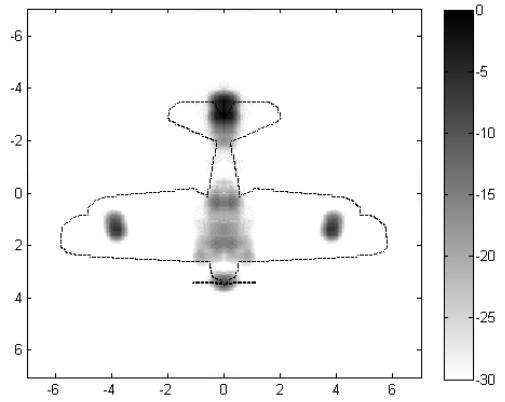

Fig. 8. Final ISAR image constructed via a wide-angle $(0° - 360°)$ backscattered data collection

4. Discussions and conclusions

In this work, a simple but an effective method for forming the wide-band wide-angle ISAR image is introduced and applied. The details of the method are given and design aspects associated with signal processing matters are discussed. The effectiveness of the algorithm is tested via a numerical example. The selected target is an airplane model whose EM simulation is carried out with a PO-SBR simulation code. After applying the proposed algorithm to the numerical data has shown a successful formation of ISAR image for the wide-angle back-scattered electric field data. This algorithm is quite faster than the traditional ISAR imaging method that calculates the 2-D imaging integral numerically. Since our method uses a series of FFT routines, it is much faster. Only drawback of our method is the resolution. Since all sub-aperture ISAR images in our algorithm uses the resolution in the small-angle sub-data set, the algorithm provides worse resolution when compared to the traditional ISAR routine that calculates the imaging integral numerically.

Since the routine is FFT-based, the image construction is almost real-time which is impossible with the conventional numerical integration based methods. Therefore, this is the main advantage of the proposed method. On the other hand, it does not provide as good resolution as the traditional methods since the resolution cell in the final image is determined by the bandwidth of the each sub-aperture which is way worse than the one that can be get via the numerical integral based wide-angle ISAR imaging techniques.

Acknowledgement:
This work is supported by Scientific Research projects of Mersin University with project grant numbers of *BAP-FBE EEM (ÖK) 2008-3 YL* and *BAP-FBE EEM (DÜ) 2008-3 YL*.

5. References

[1] C. A. Balanis, "Antenna Theory, Analysis and Design", Harper & Row, New York, USA, 1982.
[2] M. I. Skolnik, "Introduction to Radar Systems". McGraw Hill College Div, New York, USA, 1980.
[3] D. L. Mensa, "High Resolution Radar Imaging", Artech House Inc.,1981.
[4] H. Ling, K. Chou, S. Lee, "Shooting and bouncing rays: Calculating the RCS of an arbitrarily shaped cavity", IEEE Trans. Anten. Propag. AP-37: 194-205, 1989.
[5] Randolph L. Moses, Emre Ertin, and Christian Austin, "Synthetic Aperture Radar Visualization", 38th Asilomar Conference on Signals, Systems, and Computers, Pasific Grove VA, 2004.
[6] C. Özdemir, K. Chang (Ed), "Synthetic Aperture Radar The Wiley Encyclopedia of RF and Microwave Engineering", Wiley-Interscience, New York, USA, 2005.
[7] R. M. Mersereau and A. V. Openheim, "Digital reconstruction of multidimensional signals from their projections." Proc. IEEE, vol. 62, pp.1319-1338, Oct. 1974
[8] M. Gudmundson and P.-O. Anderson, "Adjacent channel interference in an OFDM system," in IEEE 46th Vehicular Technology Conf., Atlanta, GA, pp. 918–922, Apr. 1996
[9] Ausherman, D. A., Kozma, A., Walker, J. L., Jones, H. M. and Poggio, E. C. Developments in Radar Imaging, IEEE Trans. Aerosp. Electron. Syst. AES-20(4), pp. 363-400, 1984.
[10] R. B. Blackman, J. W. Tukey, "Particular Pairs of Windows", The Measurement of Power Spectra, From the Point of View of Communications Engineering. Dover, pp. 95-101, New York, USA, 1959.
[11] C. Özdemir, Rajan Bhalla, Luiz C. Trintinalia, and Hao Ling, "ASAR – Antenna Synthetic Aperture Radar Imaging", IEEE Transactions on Antennas and Propagation Vol. 46 No. 12, pp. 1845-1852, Dec. 1998

[12] J. F. Kaiser, “Nonrecursive Digital Filter Design Using the I0- sinh Window Function”, Proc. 1974 IEEE Symp. Circuits and Systems, pp. 20-23, 1974.
[13] B. Yılmaz, C.Özdemir, , “Nümerik Yöntemlerle Saçılan Alan Hesabı, 3-B Ters Yapay Açıklı Radar Görüntülerinin Elde Edilmesi ve Saçılma Merkezleri Analizi”, 4. Savunma Teknolojileri Kongresi (SAVTEK 2008), s. 259-267, Ankara, 26-27 Haziran 2008.
[14] B. Yılmaz, C. Özdemir, “Ters Yapay Açıklıklı Radar Görüntülerindeki Saçılma Merkezi Analizi Yardımıyla Büyük ve Karmaşık Platformların Radar Soğurucu Malzeme ile Kaplanarak RKA’larının Azaltılması”, URSI-TÜRKİYE’2008 Bilimsel Kongresi, Antalya, 20-22 Ekim 2008.